Control Theory

Dennis Hens (r0852264)
Nick Hosewol (r0849415)

Assignment 5: Estimation and control of two-wheel driven cart

REPORT

Academic year 2023-2024

Contents

List of Figures

1 Cart system modelling

This report implements a combined forward and feedback controller to let the cart follow a set trajectory. The necessary variables in the design process, as well as the trajectory are indicated in figure 1.

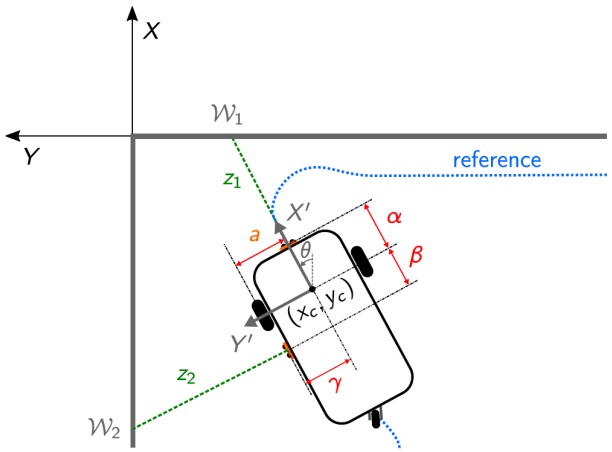

Figure 1: Schematic overview of the cart and its trajectory with indicated variables

The state of the cart on this trajectory is defined by three parameters in the state vector: $\vec{x} = [x_c, y_c, \theta]^T$, where x_c and y_c denote the coordinates of the center of the cart, expressed in the world reference frame. The axes of the world reference frame are chosen parallel with the perpendicular walls, such that the x-axis points along the front of the cart at the start of the trajectory (assuming the cart was placed correctly, of course). The y-axis points to the left of the cart. The coordinates of the center of the cart are therefore always negative, following the same convention as in assignment 3. θ denotes the angle the cart makes with the x-axis of the world reference frame.
The inputs of our system are given by the input vector $\vec{u} = [v, \omega]^T$, where v denotes the forward velocity of the cart and ω stands for the rotational velocity of the cart around its own axis. This input vector, however, cannot be controlled directly, as both wheels have to be actuated together to get the desired result. Writing down the kinematic equations for the velocities of the wheels as a function of the input yields equation 1.

$$\begin{cases} v_a &= \omega_a \cdot \frac{D}{2} = v - \omega \cdot a \\ v_b &= \omega_b \cdot \frac{D}{2} = v + \omega \cdot a \end{cases}$$
$$\iff \tag{1}$$
$$\begin{cases} v &= \frac{(\omega_a + \omega_b)D}{4} \\ \omega &= \frac{(\omega_a - \omega_b)D}{4a} \end{cases}$$

Here, $a = 0.096\,m$ is the distance from the center of the cart, and thus the center of the rotation ω to the center of the wheels. Equation 2 shows the state equation of the system. The continuous state equation is discretised immediately using the forward Euler method.

$$\begin{cases} \dot{x} &= v \cdot cos(\theta) \\ \dot{y} &= v \cdot sin(\theta) \\ \dot{\theta} &= \omega \end{cases}$$
$$\iff \tag{2}$$
$$\begin{cases} x[k+1] &= x[k] + T_s \cdot v \cdot cos(\theta) \\ y[k+1] &= y[k] + T_s \cdot v \cdot sin(\theta) \\ \theta[k+1] &= \omega[k] + T_s \cdot \omega \end{cases}$$

$T_s = 10^{-2}\,s$ is once again the sampling time of the micro-OS. These equations are inherently non-linear, due to the appearance of the sinusoidal dependence on the state θ.
Using standard trigonometric identities on figure 1, the measurements z_1 and z_2 can be projected respectively

onto the x- and y-axis, as well as the necessary given lengths, to find the exact location of x_c and y_c. Equation 3 shows the derivation of the measurement equations. In this derivation, all distances are taken to be positive, such that the values x_c and y_c turn out as negative values (which is logical, due to the definition of the world reference frame). The horizontal wall can be characterised with the equation $x = 0$ and, analogously, the vertical wall is characterised as $y = 0$. Analytically, it makes sense to start from the horizontal wall and move in the y-direction and vice versa for the vertical wall, as will be developed in the derivation. The used distances are defined in figure 1 and were measured on the cart. They equal to $\alpha = 0.075\,m$, $\beta = 0.065\,m$ and $\gamma = 0.079\,m$

$$\begin{aligned}
&\begin{cases} -z_1 \cdot cos(\theta) - \alpha \cdot cos(\theta) & = x_c \\ -z_2 \cdot cos(\theta) - \gamma \cdot cos(\theta) + \beta \cdot sin(\theta) & = y_c \end{cases} \\
&\iff \\
&\begin{cases} z_1 & = \frac{-1}{cos(\theta)}(x_c + \alpha cos(\theta)) \\ z_2 & = \frac{-1}{cos(\theta)}(y_c - \beta sin(\theta) + \gamma cos(\theta)) \end{cases}
\end{aligned} \tag{3}$$

It's evident that this equation is non-linear as well, for the same reason as earlier.

2 Design and implementation of an extended Kalman filter

The extended Kalman filter is an estimator of which the Kalman gain depends on time, with the goal of minimizing the state estimate covariance matrix at every time. An extended Kalman extends this concept for non-linear systems, using a first order Taylor series to linearise the equations using the state at every time step.
The main important assumptions of a Kalman filter still hold for the extended Kalman filter. First of all, both the measurement noise and the process noise are assumed to follow a normal distribution with mean values equal to 0, and covariance matrices respectively equal to R and Q. These statistically modeled noises are due to multiple different factors. First of all, measurement noise is created by the uncertainty of the distance sensors. This uncertainty is also dependent of the distance itself, such that this introduces even more noise. Process noise is due to the fact that the state equations are not an exact representation. Firstly, the velocities of the cart, v and ω, are assumed to be always exactly equal to their desired values. This is however not the case, as the desired velocity has to be translated by a PI-controller into control voltages first for the two DC-motors. For every step in this chain, some noise is introduced, due to modelling errors. Furthermore, process noise is also introduced when linearised equations are used, as these are approximations of the exact, non-linear system. At last, there are always some modelling errors, like not incorporating the effects of (necessary) wheel slip or (non-linear) frictional effects on the cart.

2.1 Linearisation properties of the extended Kalman filter

To linearise the equations around the current state, the Jacobi matrices of both the (non-linear) state equation and the (non-linear) measurement equation have to be known. First, equation 4 takes a look at the Jacobi matrix of the discrete time state equations. This matrix is square, as the three state equations have to be differentiated with respect to the three state variables.

$$\begin{aligned}
\frac{d\vec{f_d}}{d\vec{x}} &= \begin{bmatrix} \frac{d(x+T_s v cos(\theta))}{dx} & \frac{d(x+T_s v cos(\theta))}{dy} & \frac{d(x+T_s v cos(\theta))}{d\theta} \\ \frac{d(y+T_s v sin(\theta))}{dx} & \frac{d(y+T_s v sin(\theta))}{dy} & \frac{d(y+T_s v sin(\theta))}{d\theta} \\ \frac{d(\theta+T_s \omega)}{dx} & \frac{d(\theta+T_s \omega)}{dy} & \frac{d(\theta+T_s \omega)}{d\theta} \end{bmatrix} \\
\iff \frac{d\vec{f_d}}{d\vec{x}} &= \begin{bmatrix} 1 & 0 & -T_s v sin(\theta) \\ 0 & 1 & T_s v cos(\theta) \\ 0 & 0 & 1 \end{bmatrix}
\end{aligned} \tag{4}$$

This equation can be further solidified by computing the continuous time Jacobi matrix, and applying the continuous time Jacobi matrix to discrete time Jacobi matrix transformation, given by $\frac{d\vec{f_d}}{d\vec{x}} = I + T_s \cdot \frac{d\vec{f_c}}{d\vec{x}}$ [1].

This is shown in equation 5.

$$\begin{aligned} \frac{d\vec{f}_d}{d\vec{x}} &= I + T_s \cdot \begin{bmatrix} \frac{d(vcos(\theta))}{dx} & \frac{d(Vcos(\theta))}{dy} & \frac{d(xvcos(\theta))}{d\theta} \\ \frac{d(sin(\theta))}{dx} & \frac{d(vsin(\theta))}{dy} & \frac{d(vsin(\theta))}{d\theta} \\ \frac{d(\omega)}{dx} & \frac{d(\omega)}{dy} & \frac{d(theta+T_s\omega)}{d\theta} \end{bmatrix} \\ \iff \frac{d\vec{f}_d}{d\vec{x}} &= I + T_s \cdot \begin{bmatrix} 0 & 0 & -vsin(\theta) \\ 0 & 0 & vcos(\theta) \\ 0 & 0 & 0 \end{bmatrix} \end{aligned} \tag{5}$$

This computation yields the exact same result, as they are based on the same principle for forward Euler discretisation. Note that this Jacobi matrix correlates exactly with the A-matrix in a linear system, as will be important later on. Equation 6 shows the same derivation for the Jacobi matrix of the measurement equation. Note that, in this case, the continuous time Jacobi matrix exactly equals the discrete time Jacobi matrix, as there are no derivatives in the continuous time measurement equation that have to be discretised, using forward Euler. As there are two measurement equations dependent on three variables, this Jacobi matrix is expected to be of the size 2x3.

$$\begin{aligned} \frac{d\vec{h}_d}{d\vec{x}} &= \begin{bmatrix} \frac{d(\frac{-1}{cos(\theta)}(x+\alpha cos(\theta)))}{dx} & \frac{d(\frac{-1}{cos(\theta)}(x+\alpha cos(\theta)))}{dy} & \frac{d(\frac{-1}{cos(\theta)}(x+\alpha cos(\theta)))}{d\theta} \\ \frac{d(\frac{-1}{cos(\theta)}(y_c-\beta sin(\theta)+\gamma cos(\theta)))}{dx} & \frac{d(\frac{-1}{cos(\theta)}(y_c-\beta sin(\theta)+\gamma cos(\theta)))}{dy} & \frac{d(\frac{-1}{cos(\theta)}(y_c-\beta sin(\theta)+\gamma cos(\theta)))}{d\theta} \end{bmatrix} \\ \iff \frac{d\vec{h}_d}{d\vec{x}} &= \frac{-1}{cos(\theta)} \cdot \begin{bmatrix} 1 & 0 & \frac{xsin(\theta)}{cos(\theta)} \\ 0 & 1 & \frac{y_c sin(\theta)+\beta}{cos(\theta)} \end{bmatrix} \end{aligned} \tag{6}$$

This Jacobi matrix of the measurement equations correlates exactly to the C matrix of a linear system, and is thus implemented as such.

2.2 Properties of the extended Kalman filter

As discovered in assignment 3, the Kalman filter is a state estimator with the goal of minimizing the state covariance $\hat{P}_{k|k}$, which represents the uncertainty of the state estimate $\hat{x}_{k|k}$. As discussed earlier, the process noise and measurement noise are assumed to be strictly Gaussian, with respective covariance matrices Q and R. Even though these matrices are all actual physical properties of the system, they are often treated as design parameters, to optimize the filter in a desired way, like choosing Q extremely high to accurately track measurements despite the noise.

The easiest matrix to determine is the measurement noise covariance matrix. The cart is equipped with two measurement sensors, which both have their own measurement uncertainties. As the two sensors function independently, the covariance matrix is diagonal, with the variance of both sensors on the diagonal. As the first measurement z_1 is done by the frontal distance sensor, its variance is on the first diagonal element. The variance of the sensor on the left side is placed on the second diagonal element, while all other elements are uniquely zero.

The variances of both sensors are determined by taking a steady measurement at $z = 18\,cm$, which is the average value of the operating range of the sensor. The measurement data is then loaded into *MATLAB*. An approximation of the variance is now given by the command *var*. The measurement variance matrix R is given by equation 7.

$$R = \begin{bmatrix} 5.5990 \cdot 10^{-6}\,m^2 & 0 \\ 0 & 5.5029 \cdot 10^{-6}\,m^2 \end{bmatrix} \tag{7}$$

The initial state is set to the starting state of the swiveled cart, where $x = -30\,cm$, $y = -20\,cm$ and $\theta = 0\,rad$. The covariance matrix of this state is determined by the uncertainty introduced when manually positioning the cart, as this is how all the experiments were initiated (in contrast to assignment 3, where the positioning was done using the displacement sensor). For the linear displacements in both directions, an expected error (in one direction) of $3\,cm$ was estimated, leading to the first diagonal elements equalling $9 \cdot 10^{-4}\,m^2$. Analogously, the initial angle is estimated to have a maximal error of 3° in one direction, such that the third diagonal element equals $2.742 \cdot 10^{-3}\,rad^2$. The final initial state covariance matrix is given by equation 8.

$$\hat{P}_{0|0} = \begin{bmatrix} 9 \cdot 10^{-4}\,m^2 & 0 & 0 \\ 0 & 9 \cdot 10^{-4}\,m^2 & 0 \\ 0 & 0 & 2.742 \cdot 10^{-3}\,rad^2 \end{bmatrix} \tag{8}$$

At last, the process noise matrix is chosen on the same order as in assignment 3, $O(10^{-8})$, as these values performed the best of the tested values using the NIS and SNIS criteria. Furthermore, during the initial experiments, these values did not pose any prominent issues, like overconfidence, such that the values are set for the rest of the assignment. At last, the state equations are based on the same kinematic relations as in assignment 3, with the same underlying PI-controller and DC-motor model. Note that this does not imply anything about the process noise on the θ-state, as this was not examined in assignment 3. To not overcomplicate this choice however, the same order of magnitude for the angular displacement is chosen, as this also turned out to be accurate for the initial state covariance matrix, which was based on physical evidence.

$$Q = \begin{bmatrix} 10^{-8}\, m^2 & 0 & 0 \\ 0 & 10^{-8}\, m^2 & 0 \\ 0 & 0 & 10^{-8}\, rad^2 \end{bmatrix} \tag{9}$$

2.3 Feedforward trajectory

In this section, the trajectory the swiveled car has to follow is programmed using a feed forward controller. The states are estimated using the Kalman filter, to test the functionality of said filter. The trajectory consists of a straight path in the x-direction from $x = -30\, cm$ to $x = -15\, cm$. Then, the cart rotates by $\theta = -\frac{\pi}{2}\, rad$ (thus 90° clockwise), to the right and continues it's trajectory parallel to the y-axis. It then travels from $y = -20\, cm$ to $y = -35\, cm$. Figure 2 shows the state estimate of the cart and its 95%-confidence interval.

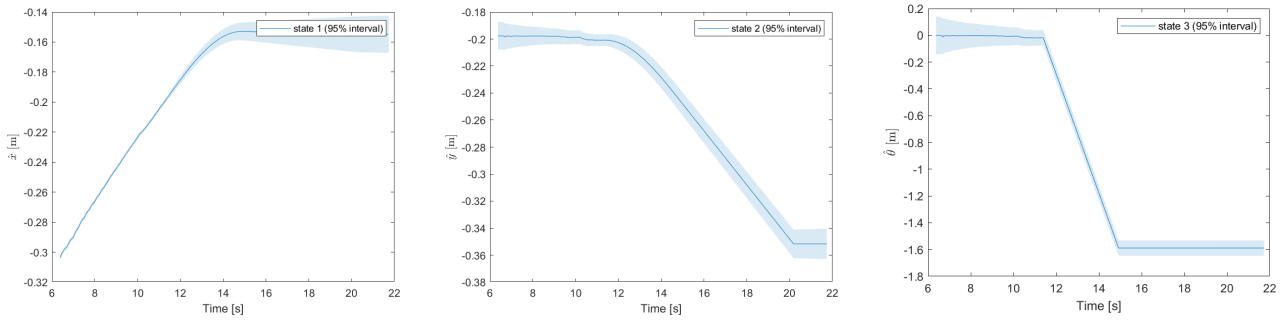

(a) Plot for $\hat{x}$ (b) Plot for $\hat{y}$ (c) Plot for $\hat{\theta}$

Figure 2: Evolution of every state in time together with its 95% confidence interval

The first plot shows the estimate on the x-state. The x-state converges almost immediately and is very certain. This is very logical as the estimate on the x-coordinate is immediately corrected by the measurement of the frontal sensor (this is helped by the fact that the initial covariance on the x-state was chosen to be very large, which leads the Kalman filter to trust the measurement more). When the turn starts, the sensors are turned off and the x-estimate has reached its supposed value of $-15\, cm$. Even though nothing happens, the uncertainty still increases. This is due to the process noise which is added once every time step. As there are no more measurements, the correction step disappears, and the uncertainty can only grow with every time step (as follows from $\hat{P}_{k+1|k} = A\hat{P}_{k+1|k}A^T + Q$).
Now as the cart drives in a straight line in the x-direction, this behaves as if it was a 1D system, thus resulting in a fast convergence. The y- and θ- uncertainties converge noticeably slower. This has to do with the fact that in the state covariance matrix, off diagonal elements appear in the $y - \theta$ spot (with other words, $P_{1|0,y\theta}$ does not equal zero). This codependence is due to the fact that the state equations are inherently linked (the link with x is not here at this point, as $\theta = 0\, rad$, thus behaving like a separate 1D system). In the correction step, the 2 uncertainties (yy and $\theta\theta$) also decrease, more significantly than in the prediction step. This can be understood in a more intuitive way: Due to the fact that there are only two measurements, it is (mathematically) impossible to uniquely determine all state variables from these measurements alone. This means by definition that the system is not observable. Using an intuitive metaphor, it's as if the measurement data of z_2 has to be shared between the y and θ states to form new estimates. This intuitively explains why the uncertainty of these states drops more slowly than the almost immediate convergence of the x-state. It's interesting to note that, if this straight line movement would continue for an infinite time, all states end up with more or less the same diagonal values. The cross covariances between y and θ never disappear.
After the sensors turn off, the y and θ uncertainties behave identically to the x state. The uncertainty starts

diverging. This also can be intuitively understood as follows: if there are no measurements, the situation is analogous to a blindfolded person trying to walk in a straight line. With every step taken, the uncertainty of where he is with respect to the line increases as every step could have a left/right deviation after all (in the analogy, the left right deviation is the process noise Q, added every step). Mathematically, turning the sensors off means that C is a zero matrix, and the correction step disappears. This indeed leads to every step just adding Q to the state covariance.

3 Design and implementation of a state feedback controller for following a position and orientation trajectory

3.1 Rotation matrix

As of now, all calculations were done in the world reference frame. To implement feedback, however, it's useful to formulate the problem in the local reference frame of the cart, which is defined as the $X'Y'$ frame in figure 1. This transformation ensures that the velocity of the cart always lies parallel to the X'-axis. The rotation ω also still lies on the Z'-axis (which points out of the screen on figure 1). The goal is to transform the tracking error vector $\hat{e}_k$ to the local reference frame, such that the state feedback can be implemented easily, as will be explained later. Due to the linearity of the rotation operator, the tracking error transforms in the same way as the coordinates themselves do (this is very obvious from the definition, as the $\hat{e}_k$ is just the difference of two coordinate vectors). As this problem is modeled as a 2D motion, the rotations always only have a component along the Z-axis. This allows for the z-component to be interpreted as a θ component, as θ coordinates transform exactly as a z-component would. (This is however not that relevant, as the Z and Z'-axes coincide anyway.)
The rotation matrix of a counterclockwise rotation with an angle $\hat{\theta}_k$, looks like equation 10. This transformation matrix transforms the coordinates of the tracking error vector from the world reference frame to the local reference frame using the equation $\hat{e}'_k = R(\hat{\theta}_k)\hat{e}_k$, where $\hat{\theta}_k$ is the instantaneous θ state and $R(\hat{\theta}_k)$ is the rotation matrix.

$$R(\hat{\theta}_k) = \begin{bmatrix} cos(\hat{\theta}_k) & sin(\hat{\theta}_k) & 0 \\ -sin(\hat{\theta}_k) & cos(\hat{\theta}_k) & 0 \\ 0 & 0 & 1 \end{bmatrix} \tag{10}$$

3.2 Static feedback matrix K

The static feedback matrix K is defined to compute the desired velocity control signals, u, from $\hat{e}'$ using the equation $u = K\hat{e}'$ and has the following structure:

$$K = \begin{bmatrix} k_x & 0 & 0 \\ 0 & k_y & k_\theta \end{bmatrix} \tag{11}$$

From this structure, the advantage of the coordinate transformation is immediately clear. If there is an error in the X' direction, which is the direction directly in front of the cart, a desired speed v, which also points along the X'-direction, as stated in the beginning of the analysis, is needed to close the gap. An error in the angle, or the Y'-direction should not contribute to this desired speed v, as, whatever value v takes, it cannot get rid of the errors in these directions. Analogously, if there is a need for a pure rotation ω, this cannot be deduced from the tracking error in the X'-direction. This, therefore explains the third zero.
To understand the other components k_y and k_θ in this row, their separate effects have to be understood first. The combination of these two factors on one line can be understood as two different controllers that 'compete' against each other to control the cart (their reactions are added, after all). If there is a tracking error in the Y'-direction, the k_y component (or controller, in the metaphor) tries to impose a rotational velocity, such that the velocity v itself starts correcting the present Y' tracking error in the next time step. Now, if there is no error in the Y'-direction, but the cart is not at the right angle (which could, roughly, occur after the previously described reaction manoeuvre), the k_θ component needs to impose a rotational velocity to restore the angle. Now, these two erros are (almost) always combined (if not in one time step, then definitely in the next one, as is clear from the correction mechanisms of both components) and have to work together to average their desired effects, such that both parameters change in a controlled manner. This can be achieved, by careful tuning of the individual feedback parameters. Note that earlier, we concluded the system is not observable. Nevertheless, this system is fully controllable. For any conceivable starting state, there exists a set of control

inputs that can guide the system to reach any final state within a finite time frame.
Now a systematic approach will be used to tune the values of k_x, k_y and k_θ. This will be done by applying the reference trajectory to the closed-loop system and varying the different values of the K-matrix. In the tuning of these parameters, no feedforward signals will be employed. Optimal values for the parameters will be determined by assessing the tracking errors of x, y and θ, as well as by evaluating the performance of the cart in following the desired trajectory, which is not always visible on the tracking error plots.

3.2.1 Tuning of k_x

As mentioned before, the value of k_x is independent of the other two values. Therefore, k_x will be tuned by setting k_y and k_θ to zero. Now three different values for k_x will be tested: 1 s^{-1}, 5 s^{-1} and 10 s^{-1}. As can be seen in figure 3a the best value for k_x is 5 s^{-1} because then the tracking error of x will converge close to zero. For $k_x = 10\ s^{-1}$ there will be an overshoot and the cart will drive too close to the wall than it should be. The response of the cart is very slow for $k_x = 1\ s^{-1}$ as can be seen in figure 3b. Because of all this k_x will be chosen to be equal to 5 s^{-1}.

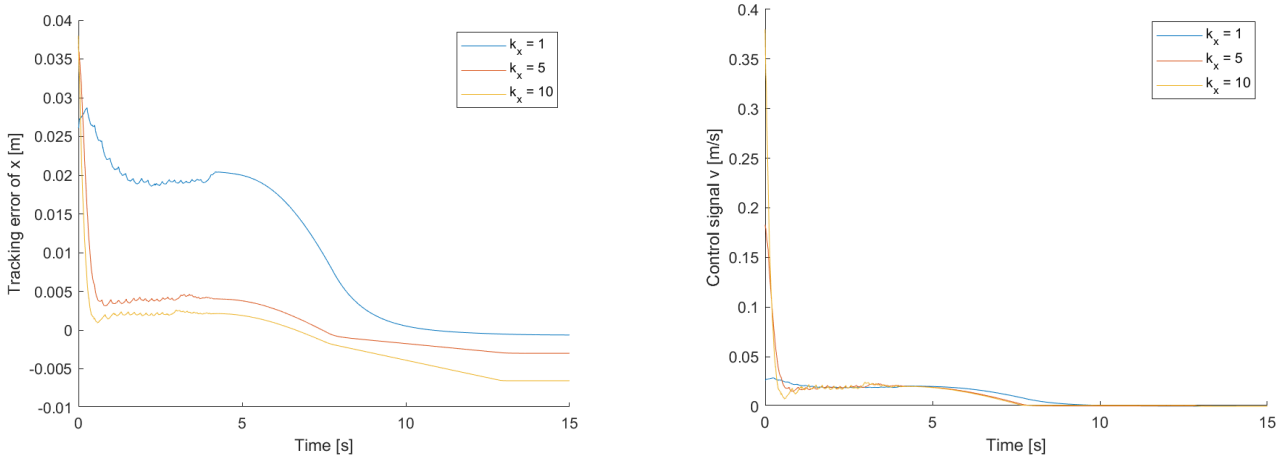

(a) Tracking error of x

(b) Control signal v

Figure 3: The tracking error of x and the control signal v in time for different values of k_x

The tracking errors of y and θ are not plotted here because these will almost be the same for different values of k_x. There is also no rotational speed ω because k_y and k_θ are zero so this control signal is also not plotted.

3.3 Tuning of k_y and k_θ

The values of k_y and k_θ are dependent on each other. Hence, the first determination will focus on whether these values should be equal or if one should be greater than the other to achieve a correct response from the system.

For this first experiment k_θ will be kept constant and equal to 1 s^{-1} and k_y will be equal to 5 $\frac{rad}{m \cdot s}$, 10 $\frac{rad}{m \cdot s}$, 25 $\frac{rad}{m \cdot s}$ and 50 $\frac{rad}{m \cdot s}$. Afterwards k_y will be constant and equal to 1 $\frac{rad}{m \cdot s}$ and k_θ will be equal to 5 s^{-1}, 10 s^{-1}, 25 s^{-1} and 50 s^{-1}. Figure 4 shows the tracking errors of y and θ for these different values of k_y and k_θ.

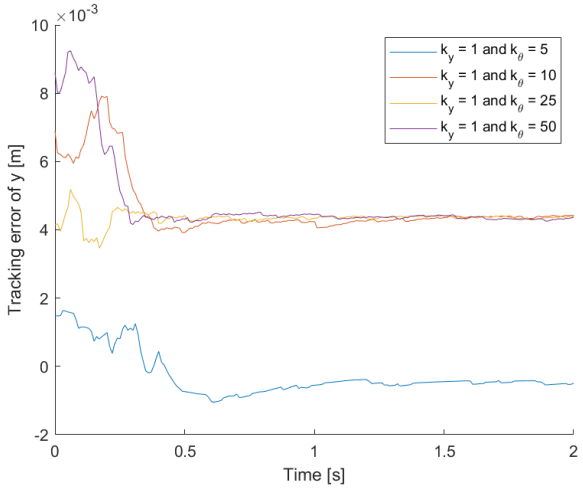

(a) Tracking error of y for $k_y = 1\ \frac{rad}{m \cdot s}$

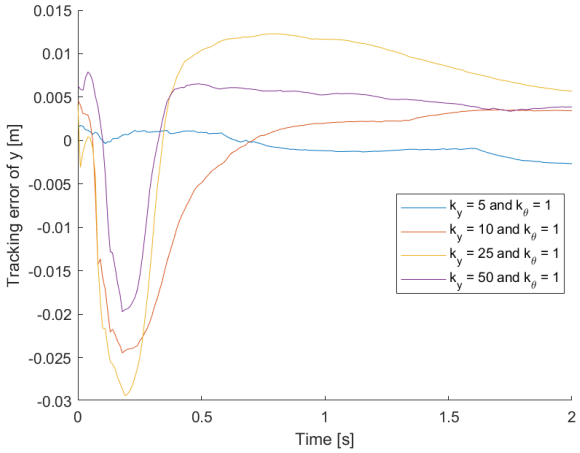

(b) Tracking error of y for $k_\theta = 1\ s^{-1}$

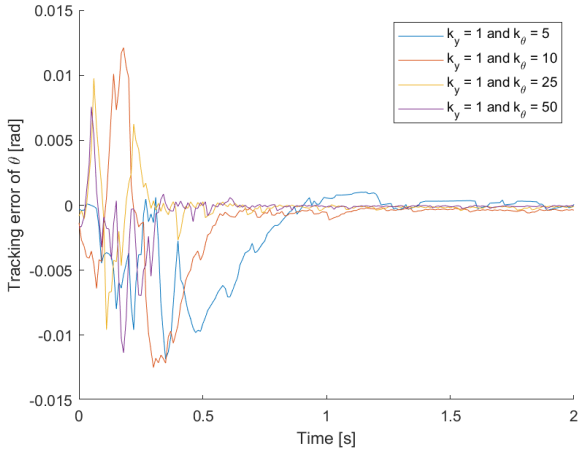

(c) Tracking error of θ for $k_y = 1\ \frac{rad}{m \cdot s}$

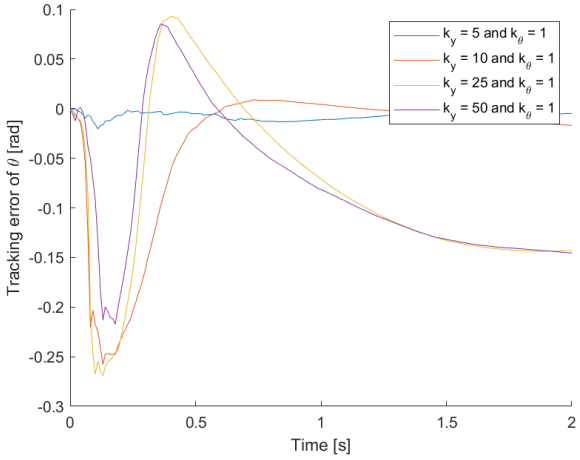

(d) Tracking error of θ for $k_\theta = 1\ s^{-1}$

Figure 4: The tracking errors of y and θ for different values of k_y and k_θ

In this experiment, it became evident that k_θ should be greater than k_y. Otherwise, the cart exhibited an unusual left turn at the start of the trajectory, causing it to move towards the left wall instead of maintaining a parallel course along that wall. This observation is illustrated in figure 4. It it clear that the errors in figures 4b and 4d are much larger than the errors in figures 4a and 4c.

Because of this observation we will now keep k_y constant and equal to $1\ \frac{rad}{m \cdot s}$ and k_θ will slightly be increased from $1\ s^{-1}$ to $9\ s^{-1}$. The error terms of y and θ are plotted again for these values in figure 5. As can be seen in the figure, the higher k_θ, the smaller the error terms during the trajectory. However, the higher the value of k_θ, the higher the overshoot of ω in the beginning (when pressing the start button), as can be seen in figure 6d. This will also increase the tracking error of θ in the beginning as can be seen in figure 5b. A higher value of k_θ will increase the rotational speed during the turn so it will complete the turn much faster. This can be seen in figure 6c, because of this, the tracking error of θ will be smaller during this turn for higher values of k_θ, this can be seen in figure 5b. Figures 6a and 6b show the control signal v in time for different values of k_θ. It is clear that v does not vary a lot for different values of k_θ.

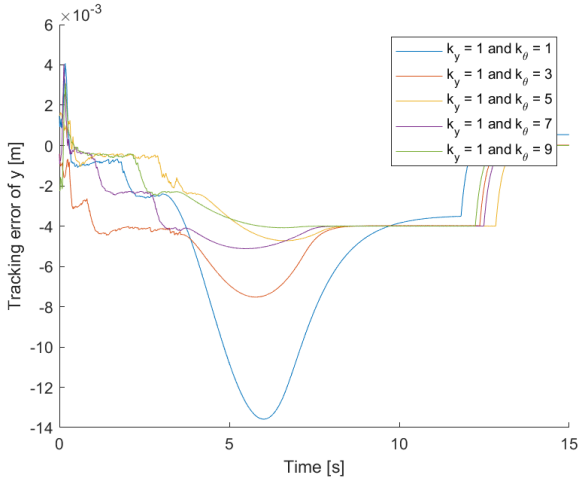

(a) Tracking error of y

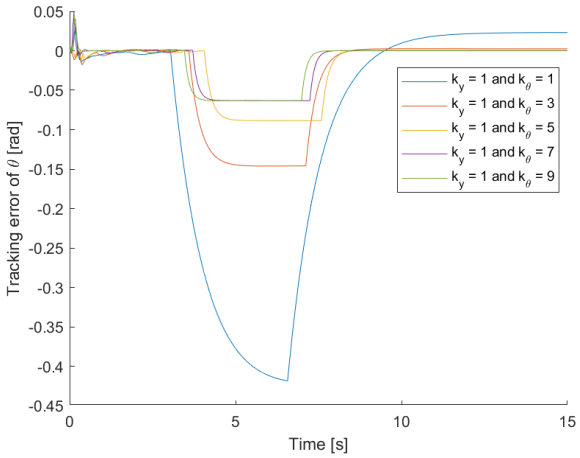

(b) Tracking error of θ

Figure 5: The tracking errors of y and θ in time when $k_y = 1\ \frac{rad}{m \cdot s}$ and k_θ varies from $1\ s^{-1}$ to $9\ s^{-1}$

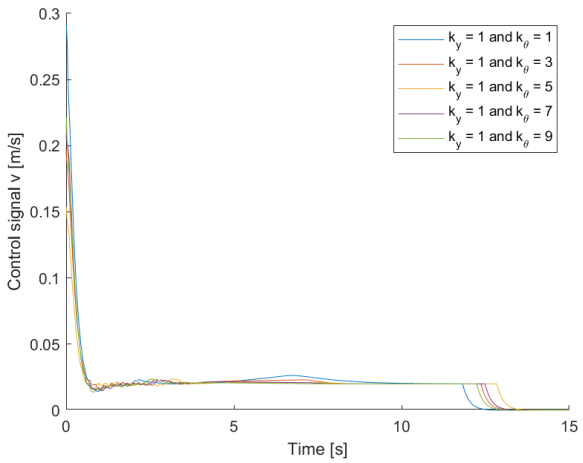

(a) Control signal v

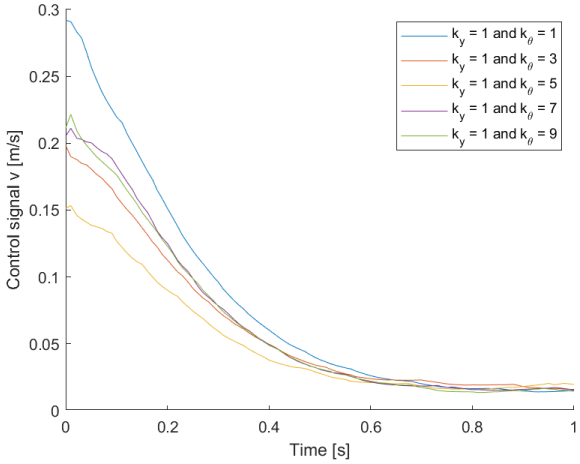

(b) Zoom of the control signal v

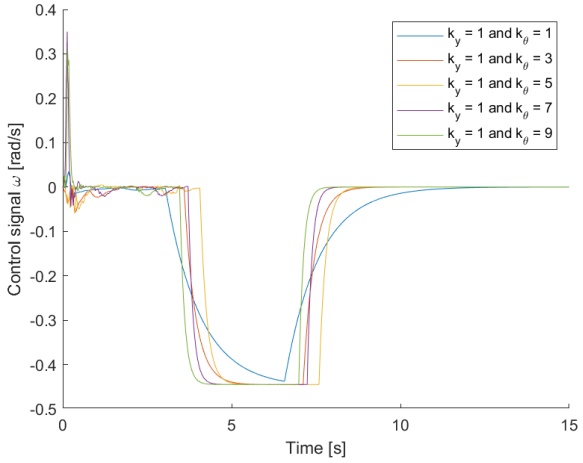

(c) Control signal ω

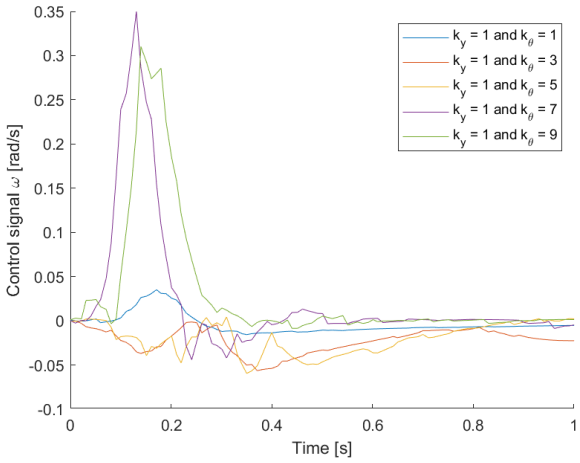

(d) Zoom of the control signal ω

Figure 6: Plot of the control signals v and ω in time when $k_y = 1\ \frac{rad}{m \cdot s}$ and k_θ varies from $1\ s^{-1}$ to $9\ s^{-1}$

The interdependence between k_y and k_θ is evident as tested before, and increasing k_θ while keeping k_y constant shows favorable characteristics, despite the mentioned drawbacks. Due to significant variations in the cart's trajectory for different parameter values, an optimal parameter set is determined through a trial-and-error

approach. Various values are selected and tested by visually tracking the cart's trajectory. If the observed trajectory appears satisfactory, further verification is conducted by plotting the tracking errors and control signals. Following this experiment, it became apparent that $k_y = 3\frac{rad}{m \cdot s}$ and $k_\theta = 7\ s^{-1}$ are optimal values. Figures 7 and 8 display the corresponding tracking errors and control signals, respectively.
As can be seen in figure 7a the tracking error of y is in the range of one the smallest tracking errors of figure 5a. The tracking error of θ is also small during the turn, as in figure 5b for the high values of k_θ, but now the tracking error in the beginning of the trajectory is much smaller than the ones in figure 5b for the high values of k_θ. This is due to the fact that k_y is increased in comparison with the previous experiment. Figure 8 shows the control signals v and ω in time. As can be seen, the cart makes the turn fast as in figure 6c for high values of k_θ, but the overshoot in the beginning is now much smaller than in figure 6d for high values of k_θ, this is due to the fact that k_y is larger than the k_y of the previous experiment.

In conclusion, it is evident that the chosen values are indeed suitable. These selected values will be employed in the subsequent stages of this assignment. The final static feedback matrix K is:

$$K = \begin{bmatrix} 5\ s^{-1} & 0 & 0 \\ 0 & 3\frac{rad}{m \cdot s} & 7\ s^{-1} \end{bmatrix} \tag{12}$$

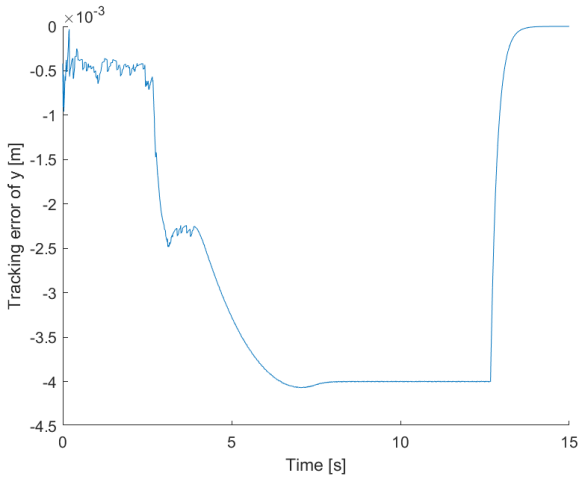

(a) Tracking error of y

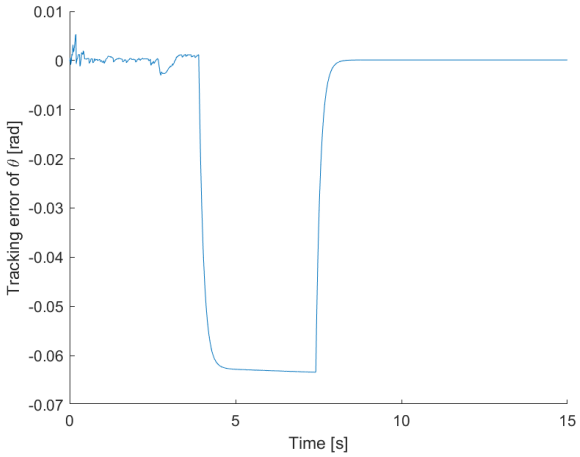

(b) Tracking error of θ

Figure 7: The tracking errors of y and θ in time when $k_y = 3\ \frac{rad}{m \cdot s}$ and $k_\theta = 7\ s^{-1}$

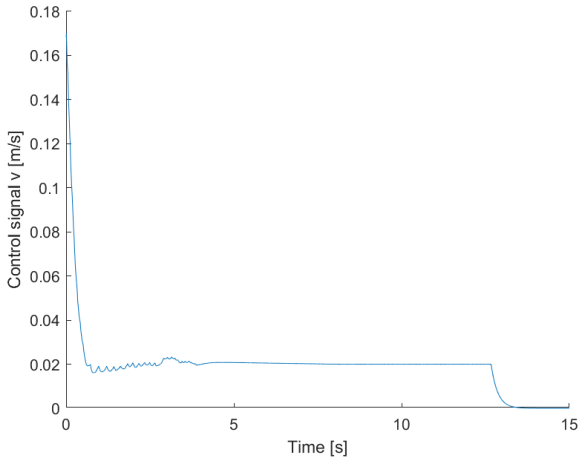

(a) Control signal v

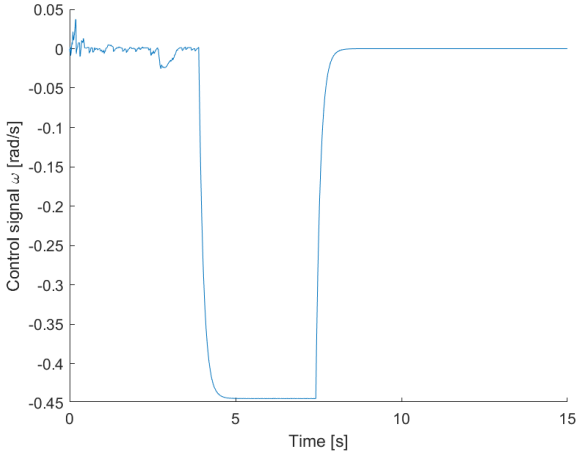

(b) Control signal ω

Figure 8: The control signals v and ω in time when $k_y = 3\ \frac{rad}{m \cdot s}$ and $k_\theta = 7\ s^{-1}$

3.4 Final state feedback controller

Finally, the tracking performance will be improved by adding the explicit feedforward signals again to the system's input: $u = u_{FF} + K\hat{e}'$. The feedforward inputs v and ω are plotted in figure 9. These feedforward inputs should be very similar to the control signals from the previous section, where only feedback was in effect (after all, they both 'force' the cart to execute the same motion). These control signals are shown in figure 8. The primary distinction lies in the initial phase of the trajectory, where there is an overshoot in the control signals for v and ω, this overshoot is absent in the feedforward inputs. The observed overshoots result from the cart not being in the desired starting position. The feedback system works to regulate and attain the desired position; without feedback, achieving this desired starting position is not possible. Additionally, the transition of a feedforward input is abrupt (as it's not based on any physical thing happening, but programmed in advance), a characteristic not observed in the changes of the control signals where these transitions are smoother (due to the fact that the input of the feedback are always based on the estimates of the physical system states).

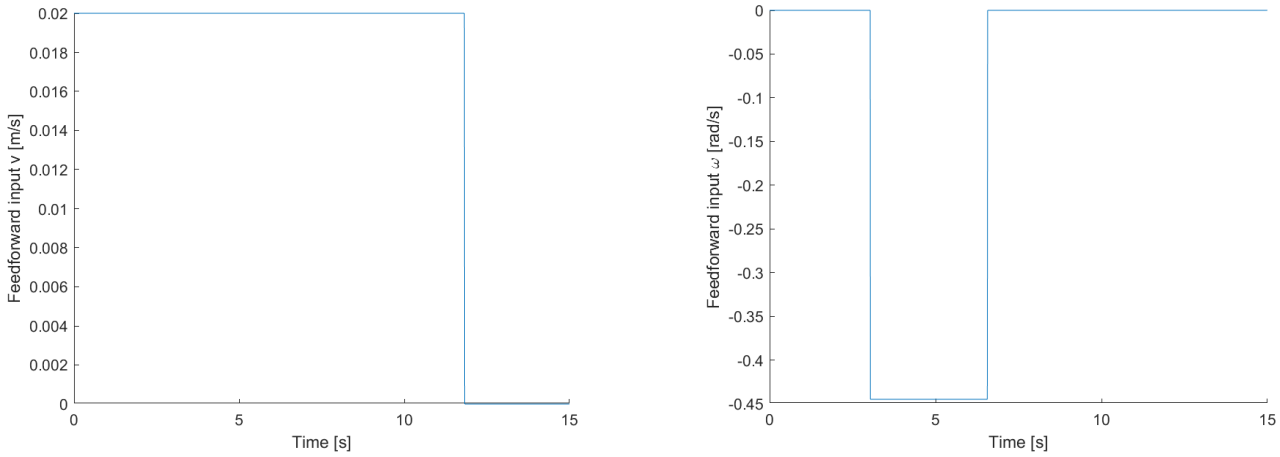

(a) Control signal v

(b) Control signal ω

Figure 9: The feedforward inputs v and ω in time

The 'complete' control signals, along with the individual contributions of feedback and feedforward inputs, are illustrated in figure 10. As can be seen, the contribution of the feedback control law is minimal to the complete control signal, with a significant impact only observed at the start of the trajectory. This peak values at the start are attributed to the cart orienting itself to the desired initial position. After this the cart will follow the desired trajectory, which was already well regulated with only the feedforward signals. The feedback control signals are only needed when the cart is not in the desired position, they serve more like a corrector, ensuring the cart realigns with the desired path in case of any positional discrepancies.

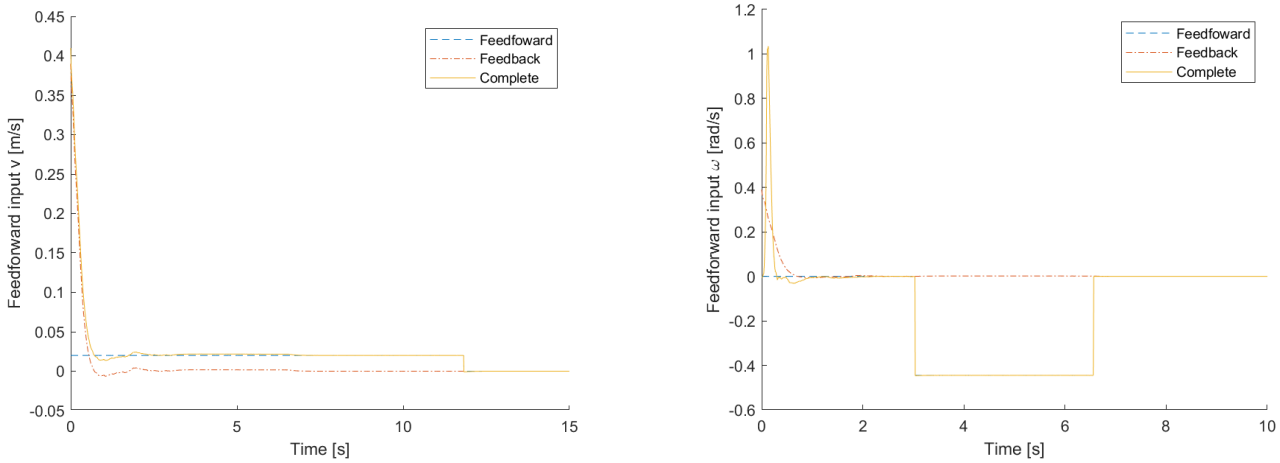

(a) Control signal v (b) Control signal ω

Figure 10: The complete control signals v and ω in time

The tracking errors of x, y and θ are plotted in figure 11. It is clear that these tracking errors are almost everywhere very close to zero. Only in the beginning of the trajectory there are some larger tracking errors. This is due to the fact that the cart is not exactly in the desired initial position. The feedback control signals will make sure the cart will start its trajectory in the desired position and so the errors will go to zero very quickly. The tracking error of y takes a bit longer to converge to zero due to the fact that both k_y and k_θ influence this error. As k_θ wants the cart to move straight, it works against the correcting action of k_y. This leads to a slower reduction of the tracking error.

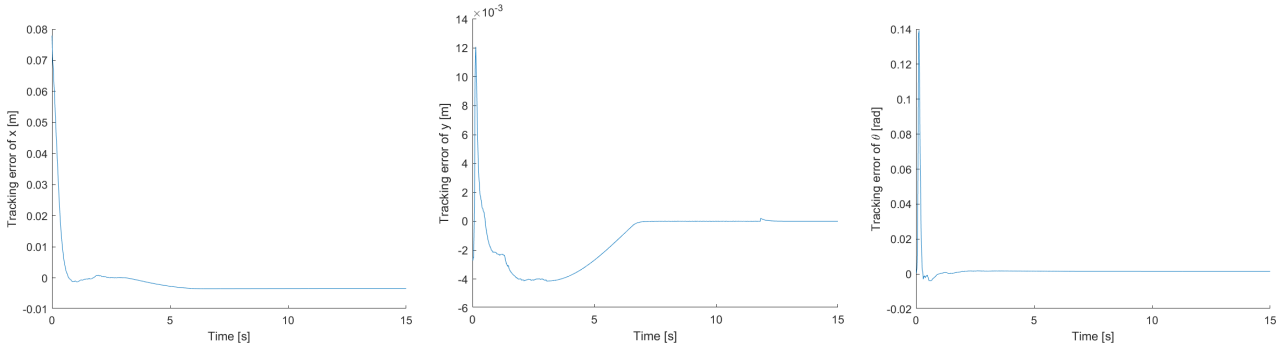

(a) Tracking error of x (b) Tracking error of y (c) Tracking error of θ

Figure 11: The tracking error of x, y and θ in time

References

[1] Pipeleers and Swevers. *Control Theory - handouts*. Aug. 2020.